J. Nano- Electron. Phys.
3 (2011) No3, P. 15-27

PACS numbers: 42.81QB, 42.82ET, 42.25. – p, 52.30. – q

TM PLASMONS IN A CYLINDRICAL SUPERLATTICES (LANS) WAVE-GUIDE STRUCTURE

***H.M. Mousa*[1], *M.M. Shabat*[2]**

[1] Physics Department, Al Azhar University, Gaza, Gaza Strip, Palestinian Authority
E-mail: H.mousa@alazhar-gaza.edu.ps

[2] Physics Department, Islamic University, Gaza, P.O. Box 108, Gaza Strip, Palestinian Authority,
E-mail: shabat@mail.iugaza.edu.ps

In this work, we have investigated theoretically the propagation characteristics of TM plasmons in a cylindrical wave-guide structure of a lateral antiferromagnetic - non magnetic superlattices (LANS) bounded by a metal. We derived the Eigenmodes equation and study the dispersion properties of transverse magnetic (TM) plasmons which propagate on the waveguide. We found that, backward TM plasmons can be tuned by adjusting the thickness of the waveguide to small reduced radius. We also found that the plasmons turn from backward to forward when the bounded material is vacuum. We also illustrated the dependence of the wave index n_x on the magnetic fraction f_1 of (LANS). Larger propagation lengths of TM plasmons are realized at small reduced radius and less magnetic material in LANS. The energy flow on the waveguide is also analyzed. We studied the dependence of the power flow on the electric permittivity of the metal ε_m. More forward plasmons are observed by increasing ε_m.

Keywords: *PLASMONS, TM WAVES, DISPERSION RELATION, WAVE-GUIDES, MAGNETIC SUPERLATTICES.*

(Received 22 May 2011, in final form 21 August 2011
published online 05 November 2011)

1. INTRODUCTION

Surface plasmons (SPs)have attracted much attention in recent years. (SPs) are electromagnetic oscillations localized at the interface between dielectric and metal materials. Controlling the propagation of light at the nanoscale is one of the challenges in photonics. (SPs) provide a key opportunity to achieve this goal, due to their relatively small decayed fields [1, 2]. (SPs) dispersion can be strongly controlled by geometry. Initial experiments on Plasmon optics were carried out at planar metal/ dielectric interfaces, demonstrating basic control of plasmons. Insulator-metal-insulator structures were investigated, and have demonstrated confinement of light though at high loss [3, 4]. The metal – insulator-metal geometries, have demonstrated lower loss, higher dispersion [5, 6]. A disadvantage of planar structures is that they only confine light in one transverse direction. Recently, coaxial waveguides composed of metal core surrounded by a dielectric cylinder and clad by a metal outer layer have been introduced, that confine light in all transverse directions [7, 8]. Rene de Waele et al. [9]

theoretically studied the dispersion of coaxial Ag/Si/Ag plasmon waveguides and demonstrated that for well-chosen geometries, modes with a negative index are observed at optical frequencies. The negative- index modes have a large propagation length than the positive- index modes depending on the dielectric thickness. Negative index has been realized in microwaves [10, 11], THz waves and optical wave-lengths [12]. Quite recently, Wang and Mittleman [13] found that a simple wire can be used as effective THz waveguide. This found the way for a wide range of new applications for THz sensing and imaging. Qing Cao et al. [14] predicted that the attenuation coefficient is reduced if a copper wires waveguide is used. This due to the huge value of the relative permittivity (-6.3×10^5) and propagation of an azimuthally polarized plasmons along the wire. Huang et al. [15] considered the wave propagation along a cylindrical nanowire waveguide made of indefinite index metamaterials. They found that the backward − wave modes can have very large effective index. These nanowires can be used as phase shifters and filters in optics and telecommunications. More work has been done in investigating the waves in multilayer's structures which composed of magnetic and non magnetic layers such as $f_e f_2/z_n f_2$ superlattice. Shabat and Mousa [16-19] discussed the propagation characteristics of nonlinear electromagnetic TE surface waves in a planer waveguide structure of a lateral antiferromagnetic/nonmagnetic superlattices (LANS) film bounded by a nonlinear dielectric cover. The non-reciprocal and bistability behaviors have been noticed. Mousa [20] studied the propagation characteristics of nonlinear TM surface waves at (LANS) film bounded by a nonlinear cover. It is found that, Magnetic fraction increases the nonlinear waves power level.
In this paper, we investigate the propagation characteristics of TM plasmons guided by an optical structure. This structure consists of a lateral antiferromagnetic/nonmagnetic superlattice (LANS) such as $f_e f_2/z_n f_2$ superlattice cylinder which bounded by a metal of electric permittivity ε_m. Superlattices are described with an effective medium theory [19-21]. Such description is valid when the wave lengths of the excitations are much longer than the superlattice period where $\beta L << 1$, where β is the magnitude of the wave vector and $L = L_1 + L_2$, is the period of the superlattice, L_1 and L_2 are the thickness of the untiferromagnetic layers and non-magnetic layers , respectively [22]. $f_1 = L_1/L_2$ and $f_2 = L_2/L$, are introduced and called the magnetic and non-magnetic fractions, respectively where.

2. DERIVATION OF THE DISPERSION RELATION

The structure geometry under consideration is shown in Fig. 1. We consider the wave propagation on a cylindrical waveguide. The axis of the waveguide is along the z direction.

The effective dielectric tensor of (LANS) is described as [23]:

$$\varepsilon^e = \begin{pmatrix} \varepsilon_\perp & 0 & 0 \\ 0 & \varepsilon_\parallel & 0 \\ 0 & 0 & \varepsilon_\perp \end{pmatrix}$$

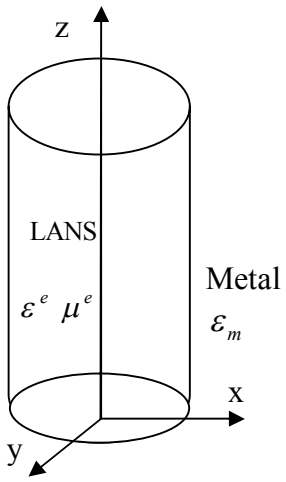

Fig. 1 *– The proposed cylindrical waveguide composed of LANS and a metal*

Where

$$\varepsilon_{\perp} = \varepsilon_1 f_1 + \varepsilon_2 f_2 \tag{1a}$$

$$\varepsilon_{\parallel} = \frac{\varepsilon_1 \varepsilon_2}{\varepsilon_1 f_2 + \varepsilon_2 f_1} \tag{1b}$$

The electric and magnetic field vectors for TM plasmons propagating along z-axis with an angular frequency ω and a wave number β will take the form [15]:

$$\begin{aligned} \vec{H} &= \vec{H}_0 \exp i(\beta z - \omega t) \\ \vec{E} &= \vec{E}_0 \exp i(\beta z - \omega t) \end{aligned} \tag{2}$$

Due to the symmetry of the waveguide, all of the field components can be expressed in terms of the longitudinal components E_z and H_z. In the polar coordinate system, by Maxwell's equations, the fields can be written inside the waveguide $r \prec a$ and outside the waveguide $r \succ a$ with a the radius of the cylinder, as:

$$H_{\varphi} = i \frac{1}{\varepsilon_{\perp} k_0^2 - \beta^2} \left(\varepsilon_{\perp} k_0 \frac{\partial E_z}{\partial r} + \beta \frac{1}{r} \frac{\partial H_z}{\partial \varphi} \right), \; r \prec a \tag{3a}$$

$$E_r = i \frac{1}{\varepsilon_{\perp} k_0^2 - \beta^2} \left(\beta \frac{\partial E_z}{\partial r} + k_0 \frac{1}{r} \frac{\partial H_z}{\partial \varphi} \right), \tag{3b}$$

$$H_{\varphi} = i \frac{1}{\varepsilon_m k_0^2 - \beta^2} \left(\varepsilon_m k_0 \frac{\partial E_z}{\partial r} + \beta \frac{1}{r} \frac{\partial H_z}{\partial \varphi} \right), r \succ a \tag{4a}$$

$$E_r = i \frac{1}{\varepsilon_m k_0^2 - \beta^2} \left(\beta \frac{\partial E_z}{\partial r} + k_0 \frac{1}{r} \frac{\partial H_z}{\partial \varphi} \right). \tag{4b}$$

The wave equations for longitudinal components inside the waveguide ($r \prec a$) are:

$$\begin{aligned} &\frac{1}{r}\frac{\partial}{\partial r}\left(r\frac{\partial E_z}{\partial r}\right)+\frac{1}{r^2}\frac{\partial^2 E_z}{\partial \varphi^2}+\varepsilon_{\|}\left(k_0^2-\frac{\beta^2}{\varepsilon_{\perp}}\right)E_z=0, \\ &\frac{1}{r}\frac{\partial}{\partial r}\left(r\frac{\partial H_z}{\partial r}\right)+\frac{1}{r^2}\frac{\partial^2 H_z}{\partial \varphi^2}+\left(\varepsilon_{\perp}k_0^2-\beta^2\right)H_z=0. \end{aligned} \tag{5}$$

The wave equations for longitudinal components outside the waveguide ($r \succ a$) are:

$$\begin{aligned} &\frac{1}{r}\frac{\partial}{\partial r}\left(r\frac{\partial E_z}{\partial r}\right)+\frac{1}{r^2}\frac{\partial^2 E_z}{\partial \varphi^2}+\left(\varepsilon_m k_0^2-\beta^2\right)E_z=0, \\ &\frac{1}{r}\frac{\partial}{\partial r}\left(r\frac{\partial H_z}{\partial r}\right)+\frac{1}{r^2}\frac{\partial^2 H_z}{\partial \varphi^2}+\left(\varepsilon_m k_0^2-\beta^2\right)H_z=0. \end{aligned} \tag{6}$$

The solutions are expressed in terms of the Bessel functions of various kinds as [24]:

$$\begin{aligned} E_z &= AJ_n\left(Kr\right)e^{in\varphi}, r \prec a \\ E_z &= CK_n\left(Rr\right)e^{in\varphi}, r \succ a \end{aligned} \tag{7a}$$

With

$$K = k_0\sqrt{\varepsilon_{\|}-\frac{\varepsilon_{\|}}{\varepsilon_{\perp}}n_x{}^2}, R = k_0\sqrt{n_x^2-\varepsilon_m} \tag{7b}$$

where $n_x = \beta/k_0$, $k_0^2 = \omega^2/c^2 = \varepsilon_o\mu_o\omega^2$, ε_0 and μ_0 are the dielectric permittivity and magnetic permeability of free space respectively, A and C are amplitude coefficients which can be determined by the boundary conditions.

For the transverse magnetic TM plasmons, $H_z = 0$, by substituting Eq.(7) into Eq.(3), the magnetic field is then obtained as:

$$\begin{aligned} H_{\varphi} &= -i\frac{\varepsilon_{\|}k_0}{K}AJ_1(Kr), r \prec a \\ H_{\varphi} &= i\frac{\varepsilon_m|k_0}{R}CK_1(Rr), r \succ a \end{aligned} \tag{8}$$

Here, we used $J_0'\left(x\right) = -J_1\left(x\right)$ and $K_0'\left(x\right) = -K_1\left(x\right)$

By using Eq.(7), The continuity of E_z at the interface $r = a$ gives:

$$\frac{C}{A} = \frac{J_n\left(Ka\right)}{K_n\left(Ra\right)} \tag{9}$$

By using Eq.(8), The continuity of H_{φ} at the interface $r = a$ gives:

$$-\frac{\varepsilon_{\|}}{K}AJ_1(Ka) = \frac{\varepsilon_m}{R}CK_1(Ra) \tag{10}$$

From recurrence relations of Bessel function, we get:

$$J_n'(x) = J_{n-1}(x) - \frac{n}{x} J_n(x) \tag{11a}$$

$$-K_n'(x) = K_{n-1}(x) + \frac{n}{x} K_n(x) \tag{11b}$$

Dividing Eq. (11a) by $xJ_n(x)$, and Eq.(11b) by $xK_n(x)$ one obtains:

$$\frac{J_n'(x)}{xJ_n(x)} = \frac{J_{n-1}(x)}{xJ_n(x)} - \frac{n}{x^2} \quad \text{and} \quad -\frac{K_n'(x)}{xK_n(x)} = \frac{K_{n-1}(x)}{xK_n(x)} + \frac{n}{x^2}.$$

Let us take the functions $g_n(x) = \frac{K_{n-1}(x)}{xK_n(x)} + \frac{n}{x^2}$ and $f_n(x) = \frac{J_{n-1}(x)}{xJ_n(x)} - \frac{n}{x^2}$.

For $n = 0,\ g_0(x) = \frac{K_{-1}(x)}{xK_0(x)}$

and $f_0(x) = \frac{J_{-1}(x)}{xJ_0(x)}$, $K_{-1}(x) = -K_1(x)$, $J_{-1}(x) = -J_1(x)$.

We obtain

$$J_1(Ka) = -KaJ_0(Ka) f_0(Ka), \quad K_1(Ra) = -RaK_0(Ra) g_0(Ra) \tag{12}$$

And

$$\frac{C}{A} = \frac{J_0(Ka)}{K_0(Ra)}. \tag{13}$$

By substituting Eq.(12) and Eq.(13) into Eq.(10), then the dispersion equation of TM plasmons is obtained as:

$$\varepsilon_{\parallel} f_0(Ka) = \varepsilon_m g_0(Ra)\ . \tag{14}$$

The existence of the solution of Eq.(14) results from the negative real value of ε_m. This negative value is due to the electron plasma contribution when the frequency is lower than the plasma frequency. This Eigen mode is called TM plasmon.

The solutions of the above dispersion equation give all the TM modes. For the mth TM band, one has $x_{0,m} \le Ka \le x_{1,m}$. Here $x_{n,m}$ is the mth zero of $J_n(x)$ away from origin. These values can be fed to Eq.(14) and corresponding Ra values are obtained. The reduced radius can be found by aid of Eq. (7b) as:

$$K^2 = \varepsilon_{\parallel}\left(k_0^2 - \frac{\beta^2}{\varepsilon_{\perp}}\right), R^2 = \beta^2 - k_0^2 \varepsilon_m \tag{15a}$$

Multiplying by a^2, then

$$(Ka)^2 = \varepsilon_{\parallel}\left((k_0 a)^2 - \frac{(\beta a)^2}{\varepsilon_{\perp}}\right), \tag{15b}$$

and

$$(Ra)^2 = (\beta a)^2 - (k_0 a)^2 \varepsilon_m, \tag{15c}$$

by substituting for $(\beta a)^2$ from Eq.(15a) into Eq.(15b). The reduced radius is:

$$k_0 a = \sqrt{\frac{(Ka)^2 \frac{\varepsilon_{\perp}}{\varepsilon_{\parallel}} + (Ra)^2}{\varepsilon_{\perp} - \varepsilon_m}}. \tag{16}$$

Once Ka and Ra values are fed into Eq.**(16),** the reduced radius is obtained. The effective index of the waveguide n_x is also evaluated by squaring Eq.(7b) and multiplying by a^2 as:

$$(Ka)^2 = (k_0 a)^2\left(\varepsilon_{\parallel} - \frac{\varepsilon_{\parallel}}{\varepsilon_{\perp}} n_x^{\,2}\right) \tag{17a}$$

and

$$(Ra)^2 = (k_0 a)^2\left(n_x^2 - \varepsilon_m\right) \tag{17b}$$

By using Eq.(17a) and Eq.(17b) then:

$$n_x = \sqrt{\frac{\varepsilon_{\parallel}(Ra)^2 + \varepsilon_m\left(Ka\right)^2}{\left(Ka\right)^2 + \frac{\varepsilon_{\parallel}}{\varepsilon_{\perp}}\left(Ra\right)^2}} \tag{18}$$

3. POWER FLOW

Inside the waveguide, $r \prec a$, by using Eq.(7a) one has:

$$E_z = AJ_0\left(Kr\right) \tag{19a}$$

By aid of Eq.(3a), Eq.(3b) and Eq.(15a), the electric field is:

$$E_r = i\frac{\varepsilon_{\parallel}\beta}{\varepsilon_{\perp}K} AJ_1(Kr), \tag{19b}$$

and the magnetic field is:

$$H_{\varphi} = i\frac{\varepsilon_{\parallel}k_0}{K} AJ_1(Kr). \tag{19c}$$

The power flow inside the waveguide is [15]:

$$P_z^{in} = \frac{1}{2}\int_0^a (E_r H_{\varphi}^* - E_{\varphi} H_r^*) r dr \tag{20}$$

By substituting Eq.(19b) and Eq.(19c) into Eq.(20), then the power flux of the plasmons propagating along the waveguide axis is

$$P_z^{in} = \frac{n_x}{2\varepsilon_\perp a^2}\int_0^a \left|\frac{J_1(Kr)}{J_1(Ka)}\right|^2 rdr \tag{21}$$

Here we set the coefficient $A = K / k_0 a\varepsilon_{\|} J_1(Ka)$.

Where $\int_0^a \left|\frac{J_1(Kr)}{J_1(Ka)}\right|^2 rdr = \frac{a\left[J_1^2(Ka)Ka - 2J_0(Ka)J_1(Ka) + J_0^2(Ka)Ka\right]}{2J_1^2(Ka)K}$ (22)

By substituting Eq.(12) and Eq.(22) into Eq.(21) we obtain:

$$P_z^{in} = \frac{n_x}{4\varepsilon_\perp K^2 a^2}\left(\frac{1}{f_0^2(Ka)} + \frac{2}{f_0(Ka)} + (Ka)^2\right)$$

Since $f_0'(Ka) = -Kaf_0^2(Ka) - \frac{2}{Ka}f_0(Ka) - \frac{1}{Ka}$, we obtain

$$P_z^{in} = -\frac{n_x}{4\varepsilon_\perp Ka}\left(\frac{f_0'(Ka)}{f_0^2(Ka)}\right) \tag{23}$$

Outside the waveguide, $r \succ a$, by using Eq.(7a) one has:

$$E_z = CK_0(Rr) \tag{24a}$$

By aid of Eq.(4a), Eq.(4b) and Eq.(15a), the electric field is:

$$E_r = i\frac{\beta CK_1(Rr)}{R}, \tag{24b}$$

and the magnetic field is:

$$H_\varphi = i\frac{\varepsilon_m k_0}{R}CK_1(Kr). \tag{24c}$$

The energy flow outside the waveguide is:

$$P_z^{out} = \frac{1}{2}\int_a^\infty (E_r H_\varphi^* - E_\varphi H_r^*)rdr. \tag{25}$$

By substituting Eq.(24b) and Eq.(24c) into Eq.(25), then the power flux of the plasmons propagating along the waveguide axis is

$$P_z^{out} = \frac{n_x}{2\varepsilon_m a^2}\int_a^\infty \left|\frac{K_1(Rr)}{K_1(Ra)}\right|^2 rdr \tag{26}$$

Here we set the coefficient $C = R / k_0 a\varepsilon_m K_1(Ra)$.

By substituting Eq.(12) into Eq.(26) we obtain :

$$P_z^{out} = \frac{n_x}{4\varepsilon_m R^2 a^2}\left(\frac{1}{g_0^2(Ra)} + \frac{2}{g_0(Ra)} - (Ra)^2\right)$$

Since $g_0'(Ra) = Rag_0^2(Ra) - \frac{2}{Ra}g_0(Ra) - \frac{1}{Ra}$, we obtain

$$P_z^{out} = -\frac{n_x}{4\varepsilon_m Ra}\left(\frac{g_0'(Ra)}{g_0^2(Ra)}\right). \tag{27}$$

The total power flow (P_z) is given as:

$$P_z = P_z^{in} + P_z^{out},$$

$$P_z = -\frac{n_x}{4\varepsilon_\perp Ka}\left(\frac{f_0'(Ka)}{f_0^2(Ka)}\right) - \frac{n_x}{4\varepsilon_m Ra}\left(\frac{g_0'(Ra)}{g_0^2(Ra)}\right).$$

The total power is normalized as [15]:

$$\langle P_z \rangle = \frac{P_z^{in} + P_z^{out}}{\left|P_z^{in}\right| + \left|P_z^{out}\right|} \tag{28}$$

Where $-1 \prec \langle P_z \rangle \prec 1$.

4. NUMERICAL RESULTS AND DISCUSSION

To compute the dispersion curves directly, and find infinite number of solutions we solve the dispersion equations numerically, this is done by feeding Ka values in the range $x_{0,m} \le Ka \le x_{1,m}$ to Eq.(14). Ra values are obtained. The obtained values of Ka and Ra can be fed to the effective wave index expression mentioned in Eq.(18).

Numerical calculations for dispersion curves are found, examples of the dispersion curves are computed for a lateral FeF_2/ZnF_2 super lattice waveguide bounded by a metal. We take the parameters as follows [22]:

$\varepsilon_1 = 5.5$ for antiferromagnetic layers, $\varepsilon_2 = 8$ for the nonmagnetic layers, $\varepsilon_m = -4$ for metal and $\varepsilon_m = 1$ for vaccum. The effective wave index n_x has been plotted versus the reduced radius of the waveguide as shown in Fig.(2a). It illustrates the first six bands of TM plasmons on the waveguide. For example, the first band's range is$(x_{0,1} \le Ka \le x_{1,1})$ of $(x_{0,1} = 1.2,$ $x_{1,1} = 1.5)$, Ra value decreases from (1.26 to 1.13), $k_0 a$ values increases from (0.05 to 0.29) and n_x values decreases from (1.2 to 0.07). The second band's range is$(x_{0,2} \le Ka \le x_{1,2})$ with $(x_{0,2} = 4.44,\ x_{1,2} = 4.6)$, Ra value decreases from (4.5 to 3.53), $k_0 a$ values increases from (0.07 to 0.92) and n_x values decreases from (1.22 to 0.03) and the third band's range is$(x_{0,3} \le Ka \le x_{1,3})$ with $(x_{0,3} = 7.56,\ x_{1,3} = 7.9)$, Ra value decreases from

(7.7 to 5.95), k_0a values increases from (0.11 to 1.55) and n_x values decreases from (1.22 to 0.07). We see that for small k_0a, TM plasmons are backward traveling as in the fist band. As k_0a increases some of them are forward traveling but the majority are backward. These waveguides can thus be used as optical buffers in integrated optical circuits. The reason is that, these waveguides support both forward and backward plasmons. Fig. 2b displays the n_x - k_0a variation for the first six TM bands, when the waveguide is (LANS) bounded by a vacuum. As we expect it shows the forward traveling waves and n_x reaches its asymptotic value quite rapidly.
As illustrated in Fig. 3a, for the first TM band, n_x has been plotted against k_0a for different magnetic fraction f_1 of the LANS waveguide. It illustrates the dependence of n_x and k_0a on the magnetic fraction. It shows that as the magnetic fraction f_1 increases to the values (0.4, 0.7 and 0.9) a large change of n_x occurs. The curves are shifted to the starting values of n_x (1.22, 1.06 and 0.94) while k_0a is stopped at the values (0.3, 0.29 and 0.27) respectively. Larger propagation lengths of TM plasmons are realized at small reduced radius and less magnetic material in LANS. This dependence of n_x on the magnetic fraction is also observed at nearly adjacent values of k_0a for forward traveling plasmons on LANS waveguide bounded by a vacuum as shown in Fig. 3b. Fig. 4a-b displays the same behaviors of the second TM band as the first TM band but the second TM band is observed at larger k_0a than the first . The effect of electric permittivity ε_m of a metal on dispersion of the second TM band is noticed in Fig. 5. It describes n_x versus k_0a for a series of decreasing negative values of electric permittivity ε_m (− 4, − 2, − 1). It displays high values of n_x and large propagation lengths which are reached by decreasing ε_m. Once the propagation characteristics are determined from the dispersion equation(14), the obtained values of the effective wave index can be fed to the power expression mentioned in Eq.(28). The normalized power $\langle P_z \rangle$ has been plotted versus the waveguide reduced radius k_0a for the first five TM bands, when the waveguide is (LANS) bounded by a metal as noticed in Fig.6. It shows that for some portion of the bands $\langle P_z \rangle$ is negative, the group velocity and the phase velocity are in opposite directions and thus plasmons are backward. For the first band, at critical radius (k_0a = 2.1) where $\langle P_z \rangle$ = 0 the group velocity is zero and the backward and forward plasmons become degenerate, the energy flow inside the waveguide cancels out that in LHM. By increasing k_0a values, the $\langle P_z \rangle$ values increase sharply to positive values until reaches the higher value of 1 where it becomes constant while k_0a values increase. This means that the waves turn to the forward propagation where energy flow and phase propagation are in the same directions. Figure 7 also describes $\langle P_z \rangle$ versus n_x of the first TM band for a series of increasing negative values of electric permittivity ε_m (− 1, − 6, − 8, − 15). It displays that by increasing of n_x, $\langle P_z \rangle$changes from negative values (backward propagation) to positive values (forward propagation). Increasing ε_m to the values (− 1, − 6, − 8, − 15) shifts the curves to starting values (− 0.59, − 0.23, − 0.18, 0.13) respectively, and more forward plasmons are observed. At ε_m = − 15, all plasmons are forward traveling.

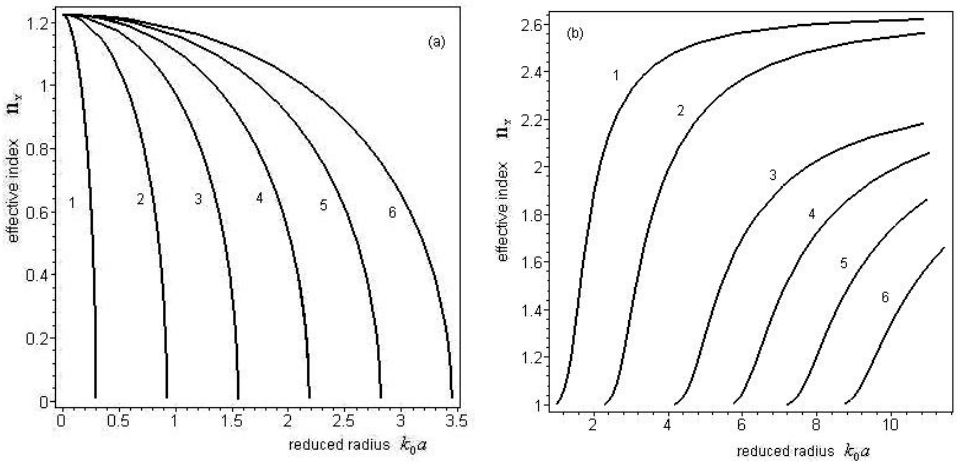

Fig. 2 *– Dispersion curves of TM plasmons for the first six bands of LANS waveguide bounded by a metal,* $\varepsilon_m = -4$*, The curves are labeled with values of,* $\varepsilon_1 = 5.5$*,* $\varepsilon_2 = 8$*, and magnetic fraction* $f_1 = 0.4$ *(a). Dispersion curves of TM guided waves for the first six bands of LANS waveguide bounded by vacuum. The curves are labeled with values of,* $\varepsilon_1 = 5.5$*,* $\varepsilon_2 = 8$*,* $\varepsilon_m = 1$ *and magnetic fraction* $f_1 = 0.4$ *(b)*

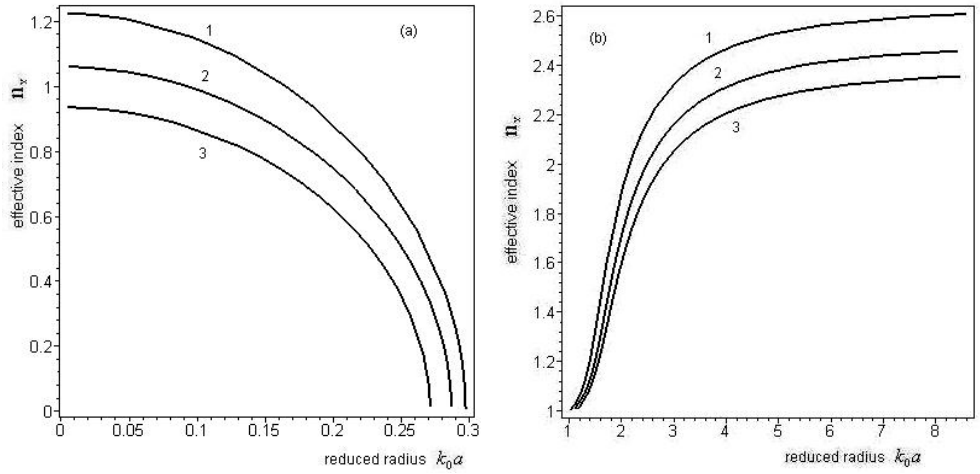

Fig. 3 *– Dispersion curves of the first band of TM plasmons of LANS waveguide bounded by a metal,* $\varepsilon_m = -4$*, for* (1) $f_1 = 0.4$*,* (2) $f_1 = 0.7$ and (3) $f_1 = 0.9$ *(a). Dispersion curves of the first band of TM guided waves of LANS waveguide bounded by vacuum for* (1) $f_1 = 0.4$*,* (2) $f_1 = 0.7$ and (3) $f_1 = 0.9$*,* $\varepsilon_1 = 5.5$*,* $\varepsilon_2 = 8$ *(b)*

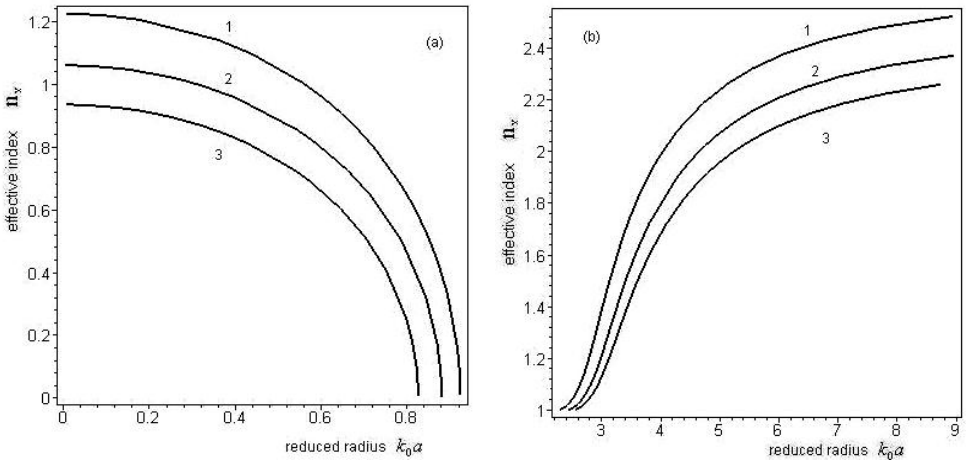

Fig. 4 *– Dispersion curves of the second band TM plasmons of LANS waveguide bounded by a metal,* $\varepsilon_m = -4$, *for* (1) $f_1 = 0.4$, (2) $f_1 = 0.7$ and (3) $f_1 = 0.9$ *(a). Dispersion curves of the second band of TM guided waves of LANS waveguide bounded by vacuum for* (1) $f_1 = 0.4$, (2) $f_1 = 0.7$ and (3) $f_1 = 0.9$, $\varepsilon_1 = 5.5$, $\varepsilon_2 = 8$ *(b)*

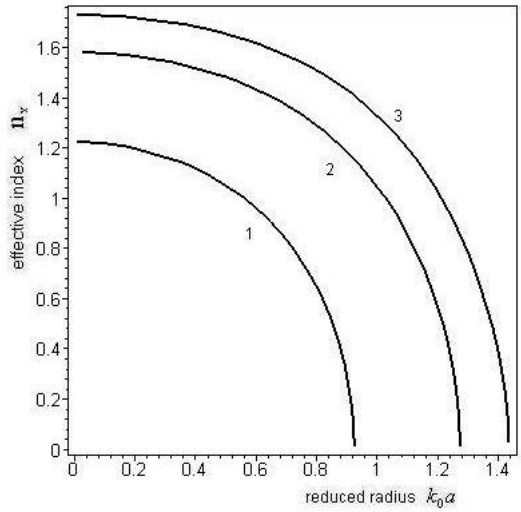

Fig. 5 *– Dispersion curves of the second band TM plasmons of waveguide bounded by a metal for* (1) $\varepsilon_m = -4$, (2) $\varepsilon_m = -2$ and (3) $\varepsilon_m = -1$, $\varepsilon_1 = 5.5$, $\varepsilon_2 = 8$, $f_1 = 0.4$

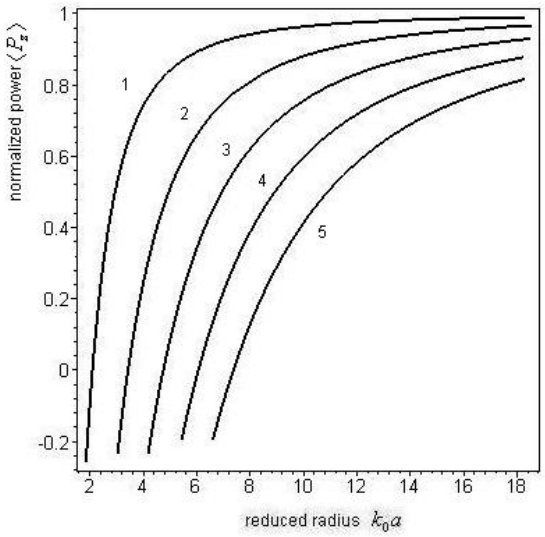

Fig. 6 *– Normalized power flow of TM plasmons as a function of the reduced radius for the first TM five bands of waveguide bounded by a metal for* $\varepsilon_m = -4$, $\varepsilon_1 = 5.5$, $\varepsilon_2 = 8$, $f_1 = 0.4$

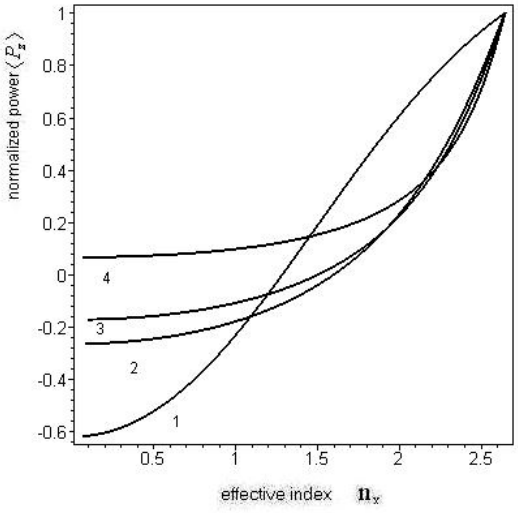

Fig. 7 *– Normalized power flow of TM plasmons as a function of the effective wave index for the first band of waveguide bounded by a metal for* (1) $\varepsilon_m = -1$, (2) $\varepsilon_m = -6$, (3) $\varepsilon_m = -8$, $\varepsilon_m = -15$, $\varepsilon_1 = 5.5$, $\varepsilon_2 = 8$, $f_1 = 0.4$

5. CONCLUSIONS

The obtained results of a new cylindrical waveguide structure containing a metal and superlattices significantly expand the possibilities of designing and constructing new optoelectronics devices and systems.

REFERENCES

1. W.L. Barnes, A. Dereux, T.W. Ebbesen, *Nature* **424**, 824 (2003).
2. E. Ozbay, *Science* **311**, 189 (2006).
3. M.I. Stockman, *Phys. Rev. Lett.* **93**, 137404 (2004).
4. E. Verhagen, A. Polman, L. Kuipers, *Opt. Express* **16**, 45 (2008).
5. J.A. Dionne, L.A. Sweatlock, H.A. Atwater, A. Polman, *Phys. Rev. B* **73**, 035407 (2006).
6. H. Miyazaki, Y. Kurokawa, *Phys. Rev. Lett.* **96**, 097401 (2006).
7. W.J. Fan, S. Zhang, B. Minhas, K.J. Malloy, S.R. J.Brueck, *Phys. Rev. Lett.* **94**, 033902 (2005).
8. F.I. Baida, A. Belkhir, D.V. Labeke, O. Lamrous, *Phys. Rev. B* **74**, 205419 (2006).
9. R. Waele, S.P. Burgos, H.A. Atwater, A. Polman, *Opt. Express* **18**, 12770 (2010).
10. C.G. Parazzoli, R.B. Greegor, K. Li, B.E.C. Koltenbah, M. Tanielian, *Phys. Rev. Lett.* **90**, 107401 (2003).
11. P.V. Parimi, W.T. Lu, P. Vodo, S. Sridhar, *Nature* **426**, 404 (2003).
12. C.M. Soukoulis, S. Linden, M. Wegener, *Science* **315**, 47 (2007).
13. K. Wang, D.M. Mittleman, *Nature* **432**, 376 (2004).
14. Q. Cao, J. Jahns, *Opt. Express* **13**, 511 (2005).
15. Y.J. Huang, W.T. Lu, S. Sridhar, *Phys. Rev. A.* **77**, 063836 (2008).
16. H.M. Mousa, M.M. Shabat, H. Khalil, D. Jager, *Proc. Of SPIE* **5445**, 274 (2003).
17. H.M. Mousa, M.M. Shabat, *Int. J. Mod. Phys. B* **19**, 4359 (2005).
18. H.M. Mousa, M.M. Shabat, *Int. J. Mod. Phys. B* **21**, 895 (2007).
19. M.M. Shabat, H.M. Mousa, *Proc. SPIE*, **6582**, 65820K (2007).
20. H.M. Mousa, *The Islamic University Journal*, **15**, 147 (2007).
21. M.C. Oliveros, N.S. Almeida, D.R. Tilley, J. Thomas, R.E. Camley, *J. Phys. Condens. Matter* **4**, 8497 (1992).
22. X. Wang, D.R. Tilley, *Phys. Lett. A* **187**, 325 (1994).
23. N.S. Almeida, D.L. Mills, *Phys. Rev. B* **38**, 6698 (1988).
24. G.N. Watson, *A Treatise on the Thoery of Bessel Functions, 2nd ed.* (Cambridge: Cambridge U. Press: 1966).